Published in final edited form as:
Mol Imaging. 2012 June ; 11(3): 187–196.

Detection of Myocardial Ischemia-Reperfusion Injury Using a Fluorescent Near-Infrared Zinc(II)-Dipicolylamine Probe and ^{99m}Tc Glucarate

Leonie wyffels[*], **Brian D. Gray**, **Christy Barber**, **Koon Y. Pak**, **Safiyyah Forbes**, **Jeffrey A. Mattis**, **James M. Woolfenden**, and **Zhonglin Liu**
Department of Radiology, University of Arizona, Tucson, AZ; Molecular Targeting Technologies, Inc., West Chester, PA; Department of Chemistry and Biochemistry, University of Notre Dame, Notre Dame, IN

Abstract

A fluorescent zinc 2,2′-dipicolylamine coordination complex PSVue®794 (probe 1) is known to selectively bind to phosphatidylserine exposed on the surface of apoptotic and necrotic cells. In this study, we investigated the cell death targeting properties of probe 1 in myocardial ischemia-reperfusion injury. A rat heart model of ischemia-reperfusion was used. Probe 1, control dye, or ^{99m}Tc glucarate was intravenously injected in rats subjected to 30-minute and 5-minute myocardial ischemia followed by 2-hour reperfusion. At 90 minutes or 20 hours postinjection, myocardial uptake was evaluated ex vivo by fluorescence imaging and autoradiography. Hematoxylin-eosin and cleaved caspase-3 staining was performed on myocardial sections to demonstrate the presence of ischemiareperfusion injury and apoptosis. Selective accumulation of probe 1 could be detected in the area at risk up to 20 hours postinjection. Similar topography and extent of uptake of probe 1 and ^{99m}Tc glucarate were observed at 90 minutes postinjection. Histologic analysis demonstrated the presence of necrosis, but only a few apoptotic cells could be detected. Probe 1 selectively accumulates in myocardial ischemia-reperfusion injury and is a promising cell death imaging tool.

TWO DISTINCT FORMS of cell death can be distinguished, necrosis and apoptosis. Apoptosis or programmed cell death is a highly regulated, active process that leads to elimination of the cell without evoking an inflammatory response. In contrast, necrosis is a disorganized, passive form of cell death, characterized by swelling and rupture of the cell membrane, resulting in activation of an inflammatory response.[1,2] Although it was initially believed that in myocardial ischemia and reperfusion, cardiomyocytes die through necrosis, it has become recognized during recent years that ischemic cell death may also occur through apoptosis.[3,4] Apoptosis may precede or occur in coexistence with the process of necrotic cell death.[5] Unlike necrosis, apoptosis is amenable to intervention. Inhibitors of the apoptotic enzymatic cascade decrease the degree of infarction in response to an ischemic insult, providing a better outcome for the patient.[6,7] Although it is clear that both forms of cell death contribute to myocardial injury following ischemia-reperfusion, the relative contribution of each remains the subject of much debate. Molecular imaging of cell death in experimental myocardial infarction is expected to permit further insight into the time course

Address reprint requests to: Zhonglin Liu MD, Department of Radiology, University of Arizona, PO Box 245067, Tucson, AZ 85724-5067; zliu@radiology.arizona.edu..
[*]Current Affiliation: University Hospital Antwerp, Antwerp (Oedeem), Belgium.

and distribution of different forms of cell death and offers an efficient tool for screening of antiapoptosis agents.

A common molecular marker for the detection of both apoptotic and necrotic cells is the exposure of phosphatidylserine (PS). In healthy cells, PS is mostly restricted to the inner leaflet of the cell membrane. Induction of apoptosis results in redistribution of phospholipids across the bilayer and consequent externalization of PS to the outer leaflet of the cell membrane.[8] This externalization of anionic PS results in a net buildup of negative charge on the membrane surface.[9] The appearance of PS on the cell membrane surface is an early sign that the cell death program has been activated[10] and serves as an “eat me” signal for phagocytosis.[11] In necrotic cells, PS is exposed to the extracellular milieu owing to passive rupture of the cell membrane. Once it becomes accessible, PS provides an abundant target for the imaging of cell death.

Annexin V is a 36 kDa physiologic protein belonging to the annexin family that selectively binds to PS in a Ca^{2+}-dependent manner. It has been conjugated to several reporter elements for in vitro[12,13] and in vivo[14–17] detection of apoptosis and necrosis. Although annexin V derivatives remain under extensive investigation, their current usefulness for in vivo detection of cell death is limited by undesirable pharmacokinetic properties and low signal to noise ratios associated with the relatively large protein-based probes.[11,18] Low-molecular-weight probes might be better tools for molecular imaging of cell death processes. Recently, Smith and colleagues discovered that rationally designed zinc 2,2′-dipicolylamine (Zn^{2+}-DPA) coordination complexes can mimic the apoptosis sensing function of annexin V.[19] Two Zn^{2+}-DPA units in *meta* position on a phenyl ring are responsible for the PS recognition and binding.[20] Fluorescent Zn^{2+}-DPA coordination complexes have been shown to selectively stain dead and dying cells that expose PS.[21,22] The focus in this study was on the Zn^{2+}-DPA coordination complex PSVue®794 (probe 1) (Figure 1). This commercially available probe consists of two Zn^{2+}-DPA units conjugated to a near-infrared carbocyanine fluorophore reporter element (excitation 794 nm, emission 810 nm). It has been demonstrated that probe 1 can stain the same cells as fluorescently labeled annexin V in cell cultures. It selectively binds to anionic surfaces of bacterial cells and can be used for fluorescence imaging of bacterial infection in living mice.[23,24] Furthermore, probe 1 can also be used for in vivo fluorescence imaging of necrotic regions within prostate and mammary tumor xenografts.[25]

D-Glucaric acid (glucarate) is a six-carbon dicarboxylic acid sugar that has been radiolabeled with ^{99m}Tc for detection of early necrosis in the heart and brain.[26–28] It has been reported that ^{99m}Tc glucarate specifically targets necrotic cells in the very early stages of myocyte injury but not apoptotic cells.[29] In acutely injured cells, the uptake of ^{99m}Tc glucarate is related to disruption of the myocyte and nuclear membranes, allowing free intracellular diffusion and electrochemical binding of the negatively charged glucarate complex to positively charged histones.[11] In ischemic cardiomyocytes, the sugar transport system might also play a role in the uptake of ^{99m}Tc glucarate in the myocardium, but tracer concentrations are not sufficient for in vivo detection by gamma imaging.[29]

The aim of the present study was to evaluate the cell death targeting properties of probe 1 in rat hearts with myocardial ischemia-reperfusion injury in comparison with ^{99m}Tc glucarate. A comparative study with a non-specific control dye was performed to identify nonspecific myocardial uptake of probe 1. Myocardial histologic studies and immunohistochemical staining to demonstrate the presence of necrosis and apoptosis were also performed.

Materials and Methods

Synthesis

PSVue®794 was provided by Molecular Targeting Technologies, Inc (West Chester, PA). A 1 mM solution of probe 1 was prepared according to the manufacturer's instructions. Control dye 2 (see Figure 1) was synthesized as previously described.[23]

^{99m}Tc Glucarate Preparation

Glucarate kits were provided by Molecular Targeting Technologies, Inc. Each kit consists of a sterile, pyrogen-free, lyophilized mixture of monopotassium glucarate tetrahydrate (12.5 mg) and stannous chloride dihydrate (0.21 mg). Kits were reconstituted according to the manufacturer's instructions by addition of 1.0 mL [^{99m}Tc] pertechnetate solution and reaction at room temperature for 15 minutes. Quality control was performed using Whatman 3MM CHR chromatography paper (Whatman International Ltd, Maidstone, Kent, UK) and MeCN:H_2O (60:40) as the mobile phase. ^{99m}Tc colloids remained at the origin and free ^{99m}Tc pertechnetate moved to the solvent front, whereas ^{99m}Tc glucarate moved with the solvent at retention factor (Rf) = 0.3. Rf = 0.3. Radiochemical purity was > 98%.

Rat Model of Myocardial Ischemia-Reperfusion

Healthy male Sprague-Dawley rats were anesthetized with an intraperitoneal injection of ketamine-xylazine combination (90 + 5 mg/kg of body weight, respectively) and orally intubated. After intubation, respiration was maintained using a volume-controlled Inspira Advanced Safety Ventilator (Harvard Apparatus, Holliston, MA) with room air. Anesthesia was maintained as needed with 0.4 to 1% isoflurane and medical grade oxygen. The chest cavity was opened and the left coronary artery (LCA) was ligated for 5 minutes (I-5) or for 30 minutes (I-30) using a 6.0 polypropylene suture. Ligation of the LCA induced an elevation of the ST segment on the electrocardiogram (ECG) and a significant increase in the QRS complex amplitude. This was observed in all rats within 5 minutes of coronary ligation.

These changes in the ECG, together with the pale appearance of the myocardium around the ligation, were used to confirm a successful ligation and the presence of regional myocardial ischemia. Subsequently, the suture was released to allow reperfusion. After reperfusion, the loose suture was left in place and the chest wall was closed in sutured layers. Buprenorphine (0.5 mg/kg; The Butler Co., Dublin, OH) was given subcutaneously for pain relief. The rats were extubated and allowed to recover from anesthesia. Two hours after reperfusion, the rats were injected intravenously with probe 1 (1.2 mg/kg body weight, 160 μL on average), immediately followed by an intravenous injection of ^{99m}Tc glucarate (approximately 110 MBq). Ninety minutes or 20 hours later, the rats were reanesthetized, and the incisions were reopened. The LCA was reoccluded and 0.6 to 0.7 mL of Evans blue (2.5% in saline, w/v) was injected into the femoral vein to delineate the myocardial ischemic area at risk. The animals were then euthanized using Beuthanasia-D (100 mg/kg, Schering-Plough Animal Health Corp., Union, NJ). The sham-operated animals were treated similarly but did not undergo ligation of the LCA. Blood was collected, and the heart and other main organs were excised for further analysis.

Experimental Groups

Two different experimental groups were defined. Group A consisted of 11 rats divided into three groups that were subjected to a sham operation (n = 3) or to 5 (I-5, n = 4) or 30 (I-30, n = 4) minutes of ischemia followed by 2 hours of reperfusion. Myocardial uptake of probe 1 and ^{99m}Tc glucarate was studied 90 minutes following ^{99m}Tc glucarate injection. In an additional four rats (n = 2, I-5 and n = 2, I-30), ^{99m}Tc glucarate uptake was studied 20 hours

postinjection. To determine nonspecific myocardial uptake of compound 1, group B rats were subjected to I-5 or I-30 followed by 2 hours reperfusion. The rats received an intravenous injection of probe 1 (160 μL of a 1 mM solution, $n = 6$ for I-5 and $n = 6$ for I-30) or control dye 2 (160 μL of a 1 mM solution, $n = 6$ for I-5 and $n = 6$ for I-30) and were sacrificed at 90 minutes postinjection (3.5 hours of reperfusion, $n = 3$, each group) or at 20 hours postinjection (22 hours of reperfusion, $n = 3$, each group).

Ex Vivo Evaluation of ^{99m}Tc Glucarate Uptake

After the animals were euthanized, the heart was quickly removed, rinsed in saline, blotted dry, and weighed. Uptake of ^{99m}Tc glucarate in the heart and blood was measured in a CRC-15W radioisotope dose calibrator/gamma well counter (Capintec, Ramsey, NJ). The uptake of radioactivity was expressed as a percentage of the injected dose per gram of tissue plus or minus the standard deviation (%ID/g tissue ± SD). Hearts were then quickly frozen to –80°C and sliced from apex to base into 2 mm thick transverse sections. Autoradiograms were obtained by exposing the heart sections to a Fujifilm phosphor imaging plate for 15 minutes. The images were then scanned at a 50 μm resolution with eight-bit pixel depth using a FujiFilm BAS5000 Bio-Imaging Analysis System and analyzed using FujiFilm Multi-Gauge 3.0 software (FujiFilm Medical Systems USA, Inc., Stamford, CT).

To demonstrate the presence of acute infarction, the heart slices were incubated in triphenyltetrazolium chloride (TTC, 1.5% solution in phosphate-buffered saline [PBS], pH 7.4) at 37°C for 20 minutes and subsequently fixed in 10% PBS-buffered formalin overnight at 2 to 8°C. TTC reacts with mitochondrial dehydrogenase in viable tissue, resulting in a deep red staining (TTC positive), whereas necrotic tissue that lacks the dehydrogenase stains a pale yellow-white (TTC negative).[30] Guided by Evans blue staining, the area at risk, which was devoid of Evans blue, was dissected from the normal myocardium. After weighing the tissues, tracer uptake (%ID/g) in the area at risk and the normal myocardium was determined by gamma counting in a well counter (Capintec).

Fluorescence Imaging

Ex vivo fluorescence signals of the heart slices were measured using a custom-built fluorescence imaging system (Department of Radiology, University of Arizona) equipped with a cooled charge-coupled device (CCD) camera (Roper VersArray CT 1300B) (Roper Scientific Inc,, Trenton, NJ) and a Schott KL 2500 LCD illuminator (Galvoptics Ltd., Basildon, Essex, UK) with a four-fiber bundle attachment. An HQ 775/50x excitation and 820 nm longpass emission filter set was used with an exposure time of 25 ms. All images were acquired under the same conditions and were comparable from day to day and animal to animal.

Images were processed and analyzed using *ImageJ* 1.43 software (National Institutes of Health, Bethesda, MD). Images were thresholded to the same absolute value. Guided by digital photographs of the Evans blue staining, regions of interest were drawn around the area at risk of the slice displaying the highest probe uptake, and mean fluorescence intensity was measured and corrected for background fluorescence. Background fluorescence intensity was determined from tissue-free regions next to the slice. The averages for compound 1 at 90 minutes ($n = 3$) and 20 hours ($n = 3$) postinjection and for control dye 2 at 90 minutes ($n = 3$) and 20 hours ($n = 3$) postinjection were calculated and plotted.

Histology

Immediately after harvesting, heart slices for histologic analysis were fixed in 10% PBS-buffered formalin overnight and then placed in 70% ethanol before processing and embedded in paraffin. Routine hematoxylin-eosin (H&E) stains were performed on 3 μm

sections of tissue cut from the formalin-fixed, paraffin-embedded blocks. The tissue preparations were examined for morphologic evidence of cell death.

Immunohistochemistry

Immunohistochemistry (IHC) was performed using rabbit anticleaved caspase-3 monoclonal antibody (mAb) (Cell Signaling Technology, Beverly, MA). Tissue sections were stained on a Discovery XT Automated Immunostainer (Ventana Medical Systems, Inc, Tucson, AZ). All steps were performed on this instrument using reagents validated by Ventana Medical Systems, including deparaffinization and cell conditioning (antigen retrieval with a borate–ethylenediaminetetraacetic acid [EDTA] buffer). Rabbit anticleaved caspase-3 mAb was detected using a biotin-free detection system (ultraView Universal DAB, VMSI #760-4515) (Ventana Medical SYstems, Inc, Tucson, AZ) based on multimer technology to obtain enhanced sensitivity and low signal to noise ratio. Tissue sections were counter-stained with hematoxylin. Following staining, slides were dehydrated through graded alcohols, cleared in xylene, and coverslipped with mounting medium. For negative controls, no primary antibody was used. Tonsil tissue was used as the positive control for cleaved caspase-3. Images were captured using an Olympus BX50 microscope with an Olympus Dp72 camera and Olympus CellSense Digital Imaging software. Images were standardized for light intensity.

Statistical Analysis

Data are expressed as mean ± SD. Unpaired *t*-test was used to compare differences between groups. A p value < .05 was considered to indicate statistical significance.

Ethics

The animal experiments were performed in accordance with the principles of laboratory animal care from the National Institutes of Health (NIH) and were approved by the Institutional Animal Care and Use Committee (IACUC) at the University of Arizona.

Results

Ex Vivo ^{99m}Tc Glucarate Uptake in Myocardial Sections

Uptake of ^{99m}Tc glucarate in myocardium with ischemia-reperfusion injury was studied in rats subjected to 5 or 30 minutes of ligation of the LCA (group A). TTC-negative areas were visible in the area at risk of myocardial section of rat hearts subjected to I-30, indicating the presence of necrosis. No TTC-negative areas could be detected in the I-5 rat model and in the sham-operated rats. The uptake of radioactivity in the area at risk versus the normal myocardium was quantified by gamma counting. Whole-heart radioactivity uptake was 0.06 ± 0.03%ID/g and 0.28 6 0.06%ID/g 90 minutes postinjection in the rats subjected to I-5 and to I-30, respectively. In the rats subjected to I-5, radioactivity uptake of 0.03 ± 0.01%ID/g and 0.14 ± 0.05%ID/g was detected in the normal myocardium and the area at risk, respectively ($p > .05$). In the rats subjected to I-30, comparable uptake was present in the normal myocardium (0.03 ± 0.01%ID/g), whereas a threefold higher uptake was present in the area at risk (0.48 ± 0.07%ID/g, $p < .001$) (Figure 2).

On autoradiography, clear focal uptake of ^{99m}Tc glucarate could be detected in the area at risk of the rat hearts subjected to I-30 (Figure 3C). In the I-5 rat model, focal ^{99m}Tc glucarate uptake was observed on autoradiograms of myocardial sections in three of four rats. In sham-operated rats, no focal uptake of ^{99m}Tc glucarate could be detected (total myocardial uptake of 0.03 ± 0.003%ID/g). At 20 hours postinjection, a total myocardial uptake of 0.02 ± 0.003%ID/g and 0.13 ± 0.004%ID/g was present in hearts subjected to I-5 and I-30, respectively. Although uptake in the area at risk (0.48 ± 0.08%ID/g) of I-30 heart

slices remained clearly visible on autoradiography, uptake in the area at risk of I-5 heart slices was minimal (0.04 ± 0.00%ID/g) and only faintly visible on autoradiograms.

Uptake Study of Compound 1 in Myocardium with Ischemia-Reperfusion Injury

Directly after autoradiography imaging of ^{99m}Tc glucarate uptake, fluorescence images of distribution of compound 1 in the myocardial sections were obtained. In hearts subjected to I-5 as well as in hearts subjected to I-30, selective fluorescence accumulation was visible in the area at risk. Uptake of probe 1 and ^{99m}Tc glucarate occurred in the area at risk with similar topography and extent (13.36 ± 5.53% versus 13.49 ± 5.48% and 37.45 ± 7.20% versus 37.38 ± 8.28%, for I-5 and I-30 hearts, respectively) (Figure 3, C and D). In sham-operated rats, no hot spot accumulation of probe 1 was visible.

To demonstrate the specificity of the fluorescence signal, I-5 and I-30 rats were injected with compound 1 and analyzed at 90 minutes or 20 hours postinjection in parallel with I-5 and I-30 rats injected with a molar equal quantity of control dye 2 (group B). For rats subjected to I-5, hot spot accumulation of compound 1 was detected in the area at risk at 90 minutes postinjection, whereas significantly ($p < .05$) lower uptake was observed in the hearts of rats injected with control dye 2 (mean fluorescence intensities (arbitrary unit, a.u.) of 116.1 ± 23.4 for 1 and 45.6 ± 32.2 for control dye 2) (Figure 4, A and C, and Figure 5). For rats subjected to I-30, selective accumulation of fluorescence could be visualized in the area at risk at 90 minutes postinjection of compound 1 as well as control dye 2 (Figure 4, B and D). Mean fluorescence intensity of compound 1 in the area at risk (125.8 ± 5.3) was 1.5-fold higher compared to control dye 2 (83.4 ± 25.3). At 20 hours postinjection, hot spot accumulation of compound 1 remained detectable in the area at risk of all the hearts subjected to I-30, whereas hot spot accumulation of control dye 2 could be detected in only one of three I-30 hearts. Only faint uptake of control dye 2 was detectable in the area at risk of the other two I-30 hearts (Figure 4, F and H). Mean fluorescence intensity in the area at risk of I-30 hearts at 20 hours postinjection was 2.3-fold higher for compound 1 (56.9 ± 8.1) compared to control dye 2 (24.6 ± 16.4). For hearts subjected to I-5, hot spot accumulation of compound 1 at 20 hours postinjection could be detected in two of three hearts. No or only faint uptake was found for control dye 2 (Figure 4, E and G).

Histopathology

Heart sections (3 μm) were histopathologically analyzed with H&E staining. In the I-5 rat model, no morphologic evidence of cell damage was present (Figure 6A). In the heart sections of rats subjected to I-30, H&E staining clearly demonstrated the presence of cell damage in the area at risk, characterized by contraction bands, wavy fibers, congestion of red blood cells, and, in some areas, polymorphonuclear cell infiltration, indicating early inflammation (Figure 6C).

Following cleaved caspase-3 immunostaining, a high proportion of active caspase-3-positive cells, indicated by brown color staining, could be detected in I-5 and I-30 myocardial slices. However, the nuclear morphology of most cells was not consistent with apoptosis, and positively stained cells were also found in the viable myocardium. In the heart section of rats subjected to I-5 and 3.5 or 22 hours of reperfusion, only rare cells displaying the nuclear phenotype related to apoptosis were observed in the area at risk. More apoptotic cells were observed in the area at risk of the I-30 myocardial sections with 3.5 or 22 hours of reperfusion, but their number remained low in all the analyzed sections. Also, in myocardial slices of sham-operated rats, positive staining of mainly endothelial nuclei could be observed. However, none of the stained cells were undergoing apoptosis and the number of stained cells was much lower than in the ischemia-reperfusion heart sections. In negative

controls, no staining could be detected, whereas in positive controls, only true apoptotic cells were stained.

Discussion

Cell death in myocardial ischemia-reperfusion injury results from two different but closely related processes, apoptosis and necrosis. Molecular imaging of cell death is a useful tool for monitoring disease course and for the evaluation of therapeutic strategies aimed at limiting the amount of tissue damage in patients with myocardial infarction.

In the present study, the targeting properties of a fluorescent near-infrared zinc(II)-dipicolylamine probe PSVue®794 were evaluated in an experimental model of myocardial ischemia-reperfusion injury. Our results show that probe 1 can target ischemia-reperfusion injury and is clearly visible in the slices of hearts subjected to 5 or 30 minutes ligation of the LCA, up to 20 hours post-injection or 22 hours of reperfusion.

Probe 1 was coinjected with ^{99m}Tc glucarate to compare topography and investigate the preference of probe 1 for apoptotic or necrotic tissue. Our study confirms the preferential retention of ^{99m}Tc glucarate in acute necrotic tissue in ischemia-reperfusion injury. Given that no histopathologic evidence of cell damage or TTC-negative tissue was present in the rat hearts subjected to 5 minutes ligation of the LCA, ^{99m}Tc glucarate uptake in the I-5 myocardial slices is most likely associated with myocardial damage through placement of the suture and an upregulation of sugar transporters. Although visible by autoradiography at 90 minutes, tracer concentrations in the I-5 rat hearts are likely not sufficient for in vivo imaging.

The uptake of probe 1 in the area at risk in I-5 and I-30 myocardial slices at 90 minutes postinjection was comparable in topography and extent to the uptake of ^{99m}Tc glucarate. Although ^{99m}Tc glucarate uptake was only minimally detectable in the area at risk of I-5 hearts at 20 hours postinjection, hot spot accumulation of probe 1 was still visible at 20 hours postinjection. Given that 5 minutes ligation of the LCA does not result in necrosis, as evident from TTC and H&E staining, uptake of probe 1 is probably related to affinity for apoptotic cells. In the I-30 model, on the other hand, the uptake is likely related to a mixture of apoptotic and necrotic cardiomyocyte death because ischemia-reperfusion injury is not an all-or-none phenomenon but consists of a mixture of both reversibly and irreversibly injured myocytes. This suggests that probe 1 shows affinity for both apoptotic and necrotic cells and might explain the observation of the similar uptake pattern for probe 1 and ^{99m}Tc glucarate.

Immunohistologic analysis of the myocardial slices was performed to relate the uptake of probe 1 to apoptosis and necrosis. Many laboratories apply the terminal deoxynucleotidyl transferase–mediated dUTP-biotin neck-end labeling (TUNEL) assay for the detection of apoptosis-associated DNA strand breaks in cultured cells and tissue sections. Unfortunately, the method is not specific because it also detects nonspecific DNA degradation. DNA fragmentation is not restricted to apoptosis but also occurs in tissue autolysis and necrosis.[31] We therefore chose to use immunohistochemical staining of cleaved (activated) caspase-3 for the detection of apoptosis in the myocardial sections. Caspase-3 plays a central role in the execution phase of apoptosis by controlling DNA fragmentation and morphologic changes of apoptosis.[32] Experimental work has shown a prominent role of activated caspase-3 in cardiomyocyte death in the ischemic-reperfused myocardium.[33] Rabbit anticleaved caspase-3 mAb detects the activated form of caspase-3 by specifically recognizing the large fragment (17–19 kDa) that results from cleavage adjacent to Asp175 and is present only in cells with an initiated apoptosis process.[34]

In the present study, positively stained cells were observed not only in the area at risk of I-5 and I-30 heart sections but also in nonischemic surrounding myocardium. The rabbit anticleaved caspase-3 mAb seems to be staining a cell population of interstitial and myocardial cells that have not (or at least not yet) undergone fragmentation. Staining of normal cells was also observed in the sham-operated rats, but their number was much lower compared to the ischemic-reperfused heart sections. The staining of a normal cell population might be related to cross-reaction of the mAb with another protein or reaction with noncleaved caspase-3. Given that the proportion of caspase-3 positive cells was much higher in the ischemic-reperfused hearts, a relationship between positive staining and ischemia-reperfusion seems very likely. Only a small fraction of the positive cells displayed the nuclear morphology characteristic of apoptosis. These true apoptotic cells were present in the area at risk, and most of them were present in the I-30 myocardial sections. No true apoptotic cells could be detected in the sham-operated rats. Proper quantification of apoptotic cardiomyocytes requires a large number of sections because the number of apoptotic cells may be very small and highly variable in different parts of the sample.[1] This was beyond the scope of the present study. In previously reported studies using TUNEL or cleaved caspase-3, the proportion of apoptotic cells in the ischemic area has been highly variable. Kenis and colleagues demonstrated that even after brief periods of ischemia, even when no histologic evidence of apoptosis or necrosis is observed in the hearts, the apoptosis program is initiated with exposure of PS and activation of caspase-3.[5] Furthermore, their experiments indicate recovery from apoptosis in vivo following reperfusion, despite activation of caspase-3. This might explain why in our study cells stained positive for cleaved caspase-3, whereas only a fraction of the positive cells displayed nuclear fragmentation. Even though our study indicates targeting of apoptosis and necrosis, we cannot exclude the fact that part of the uptake of probe 1 is related to binding to other (negatively charged) cell components that can be exposed in ischemiareperfusion injury.

Although vascular hyperpermeability is known to be associated with reperfused myocardial infarct,[35] minimal washout of ^{99m}Tc glucarate from the area at risk in hearts subjected to I-30 might suggest that passive diffusion plays only a minor role in the uptake of ^{99m}Tc glucarate in the infarcted tissue. Given that uptake of ^{99m}Tc glucarate in the hearts subjected to I-5 was much more associated with washout, we speculate that accumulation of ^{99m}Tc glucarate in the area at risk of hearts subjected to I-5 min is not associated with specific binding to myocardial ischemia-reperfusion injury. The comparative experiment with nonspecific control dye 2 indicates that part of the uptake of probe 1 in the area at risk is due to passive leakage related to vascular hyperpermeability. Still, high accumulation of control dye 2 in the area at risk could be detected only at 90 minutes postinjection in the I-30 model. The higher fluorescence intensities measured for control dye 2 in the I-30 hearts compared to the I-5 hearts suggest that the nonspecific leakage of the tracer is greater following 30 minutes ligation of the LCA, presumably because of greater extent of myocardial damage. At 20 hours postinjection and in the I-5 hearts, uptake of control dye 2 was only faintly visible in most heart slices, whereas uptake of probe 1 was more defined with hot spot accumulation in the area at risk and significant higher fluorescence intensity. This indicates that the uptake of probe 1 is more likely to be associated with specific binding to cell death processes rather than nonspecific leakage.

Conclusion

We have demonstrated that it is feasible to detect ischemia-reperfusion injury with fluorescent near-infrared zinc(II)-dipicolylamine probe 1. Comparison with ^{99m}Tc glucarate uptake and histologic and immunohistochemical analysis suggests that probe 1 targets apoptotic as well as necrotic cell death in myocardial ischemia-reperfusion injury. The control study with a nonspecific dye indicates that, besides specific binding, diffuse leakage

owing to hyperpermeability contributes to accumulation of probe 1 in the area at risk. This study indicates that probe 1 may serve as an entry point to the preparation of clinically useful myocardial cell death imaging probes. It should be feasible to develop radiolabeled analogues of probe 1 for noninvasive detection of cell death processes.

Acknowledgments

We would like to thank Dr. Art Gmitro and Dr. Bradley Smith for useful discussions. Dr. Roel Van Holen is gratefully acknowledged for help with image processing. We thank Dr. Ray Nagle for stimulating discussions on the immunohistologic data and Edward Abril from Tissue Acquisition and Cellular/Molecular Analysis Shared Service (TACMASS), which is supported by an Arizona Cancer Center Support Grant (NIH CA023074), for generating the immunohistochemical and histologic data.

Financial disclosure of authors: This study was supported by NIH grants NHLBI R01-HL090716 and NIBIB P41-EB002035 and the Walther Cancer Foundation. Dr. Koon Y. Pak is an employee and shareholder of Molecular Targeting Technologies, Inc. Dr. Jeffrey A. Mattis and Dr. Brian Gray are employees of Molecular Targeting Technologies, Inc.

Financial disclosure of reviewers: None reported.

References

1. Saraste A, Pulkki K. Morphological and biochemical hallmarks of apoptosis. Cardiovasc Res. 45:528–37. 200. doi:10.1016/S0008-6363(99)00384-3. [PubMed: 10728374]
2. Krijnen PAJ, Nijmeijer R, Meijer CJLM, et al. Apoptosis in myocardial ischaemia and infarction. J Clin Pathol. 2002; 55:801–11. doi:10.1136/jcp.55.11.801. [PubMed: 12401816]
3. McCully JD, Wakiyama H, Hsieh Y, et al. Differential contribution of necrosis and apoptosis in myocardial ischemia-reperfusion injury. Am J Physiol Heart Circ Physiol. 2004; 286:H1923–35. doi:10.1152/ajpheart.00935.2003. [PubMed: 14715509]
4. Whelan RS, Kaplinskiy V, Kitsis RN. Cell death in the pathogenesis of heart disease: mechanisms and significance. Annu Rev Physiol. 2010; 72:19–44. doi:10.1146/annurev.physiol.010908.163111. [PubMed: 20148665]
5. Kenis H, Zandbergen HR, Hofstra L, et al. Annexin A5 uptake in ischemic myocardium: demonstration of reversible phosphatidylserine externalization and feasibility of radionuclide imaging. J Nucl Med. 2010; 51:259–67. doi:10.2967/jnumed.109.068429. [PubMed: 20124049]
6. Yaiota H, Ogawa L, Maehara K, et al. Attenuation of ischemia/reperfusion injury in rats by a caspase inhibitor. Circulation. 1998; 97:276–81. [PubMed: 9462530]
7. Gao F, Tao L, Yan W, et al. Early anti-apoptosis treatment reduces myocardial infarct size after a prolonged reperfusion. Apoptosis. 2004; 9:553–9. doi:10.1023/B:APPT.0000038035.75845.ab. [PubMed: 15314283]
8. Blankenberg FG. In vivo detection of apoptosis. J Nucl Med. 2008; 49:81S–95S. doi:10.2967/jnumed.107.045898. [PubMed: 18523067]
9. Hanshaw RG, Smith B. New reagents for phosphatidylserine recognition and detection of apoptosis. Biorg Med Chem. 2005; 13:5035–42. doi:10.1016/j.bmc.2005.04.071.
10. Martin SJ, Reutelingsperger CPM, McGahon AJ, et al. Early redistribution of plasma membrane phosphatidylserine is a general feature of apoptosis regardless of the initiation stimulus: inhibition by overexpression of Bcl-2 and Abl. J Exp Med. 1995; 182:1545–56. doi:10.1084/jem.182.5.1545. [PubMed: 7595224]
11. De Saint-Hubert M, Prinsen K, Mortelmans L, et al. Molecular imaging of cell death. Methods. 2009; 48:178–87. doi:10.1016/j.ymeth.2009.03.022. [PubMed: 19362149]
12. Vermes I, Haanen C, Steffens-Nakken H, et al. A novel assay for apoptosis: flow cytometric detection of phosphatidylserine expression on early apoptotic cells using fluorescein labelled annexin V. J Immunol Methods. 1995; 184:39–51. doi:10.1016/0022-1759(95)00072-I. [PubMed: 7622868]
13. van Genderen H, Kenis H, Lux P, et al. In vitro measurement of cell death with the annexin A5 affinity assay. Nat Protoc. 2006; 1:363–7. doi:10.1038/nprot.2006.55. [PubMed: 17406257]

14. Tait JF, Smith C, Levashova Z, et al. Improved detection of cell death in vivo with annexin V radiolabeled by site-specific methods. J Nucl Med. 2006; 47:1546–53. [PubMed: 16954565]
15. Yang S, Attipoe S, Klausner AP, et al. In vivo detection of apoptotic cells in the testis using fluorescence labeled annexin V in a mouse model of testicular torsion. J Urol. 2006; 176:830–5. doi:10.1016/j.juro.2006.03.073. [PubMed: 16813956]
16. van Tilbor GA, Vucic E, Strijkers GJ, et al. Annexin A5-functionalized bimodal nanoparticles for MRI and fluorescence imaging of atherosclerotic plaques. Bioconj Chem. 2010; 21:1794–803. doi: 10.1021/bc100091q.
17. Thimister PW, Hofstra L, Liem IH, et al. In vivo detection of cell death in the area at risk in acute myocardial infarction. J Nucl Med. 2003; 44:391–6. [PubMed: 12621005]
18. Bauwens M, De Saint-Hubert MD, Devos E, et al. Site-specific 68Ga-labeled annexin A5 as a PET imaging agent for apoptosis. Nucl Med Biol. 2011; 38:381–92. doi:10.1016/j.nucmedbio. 2010.09.008. [PubMed: 21492787]
19. Koulov AV, Hanshaw RG, Stucker K, et al. Biophysical studies of a synthetic mimic of the apoptosis-detecting protein annexin V. Isr J Chem. 2005; 45:373–9. doi:10.1560/6AD4-LC9G-P57M-BE5Y.
20. Lakshmi C, Hanshaw RG, Smith BD. Fluorophore-linked zinc (II) dipicolylamine coordination complexes as sensors for phosphatidylserine-containing membranes. Tetrahedron. 2004; 60:11307–15. doi:10.1016/j.tet.2004.08.052.
21. Hanshaw R, Lakshmi C, Lambert T, et al. Fluorescent detection of apoptotic cells by using zinc coordination complexes with a selective affinity for membrane surfaces enriched with phosphatidylserine. Chem Biol Chem. 2005; 6:2214–20.
22. DiVittorio K, Johnson J, Johansson E, et al. Synthetic peptides with selective affinity for apoptotic cells. Org Biorg Chem. 2006; 4:1966–76. doi:10.1039/b514748d.
23. Leevy WM, Gammon ST, Jiang H, et al. Optical imaging of a bacterial infection in living mice using a fluorescent near-infrared molecular probe. J Am Chem Soc. 2006; 128:16476–7. doi: 10.1021/ja0665592. [PubMed: 17177377]
24. Leevy WM, Gammon ST, Johnson JR, et al. Noninvasive optical imaging of Staphylococcus aureus bacterial infection in living mice using a bis-dipicolylamine-zinc (II) affinity group conjugated to a near-infrared fluorophore. Bioconj Chem. 2008; 19:686–92. doi:10.1021/ bc700376v.
25. Smith BA, Akers WJ, Leevy WM, et al. Optical imaging of mammary and prostate tumors in living animals using a synthetic near infrared zinc (II)-dipicolylamine probe for anionic cell surfaces. J Am Chem Soc. 2009; 132:67–9. doi:10.1021/ja908467y. [PubMed: 20014845]
26. Narula J, Petrov A, Pak KY, et al. Very early noninvasive detection of acute experimental nonreperfused myocardial infarction with Tc-99m-labeled glucarate. Circulation. 1997; 95:1577–84. [PubMed: 9118528]
27. Okada D, Johnson G, Liu ZL, et al. Early detection of infarct in reperfused canine myocardium using Tc-99m-glucarate. J Nucl Med. 2004; 45:655–64. [PubMed: 15073263]
28. Yaoita H, Uehara T, Brownell A, et al. Localisation of technetium-99m-glucarate in zones of acute cerebral injury. J Nucl Med. 1991; 32:272–8. [PubMed: 1704054]
29. Khaw B, Nakazawa A, O'Donnell S, et al. Avidity of technetium 99m glucarate for the necrotic myocardium: in vivo and in vitro assessment. J Nucl Cardiol. 1997; 4:283–90. doi:10.1016/ S1071-3581(97)90105-7. [PubMed: 9278874]
30. Takashi E, Ashraf M. Pathologic assessment of myocardial cell necrosis and apoptosis after ischemia and reperfusion with molecular and morphological markers. J Mol Cell Cardiol. 2000; 32:209–24. doi:10.1006/jmcc.1999.1067. [PubMed: 10722798]
31. Jakob S, Corazza N, Diamantis E, et al. Detection of apoptosis in vivo using antibodies against caspase-induced neo-epitopes. Methods. 2008; 44:255–61. doi:10.1016/j.ymeth.2007.11.004. [PubMed: 18314057]
32. Bressenot A, Marchal S, Bezdetnaya L, et al. Assessment of apoptosis by immunohistochemistry to active caspase-3, active caspase-7, or cleaved PARP in monolayer cells and spheroid and subcutaneous xenografts of human carcinoma. J Histochem Cytochem. 2009; 54:289–300. [PubMed: 19029405]

33. Holly TA, Drincic A, Byun Y, et al. Caspase inhibition reduces myocyte cell death induced by myocardial ischemia and reperfusion in vivo. J Mol Cell Cardiol. 1999; 31:1709–15. doi:10.1006/jmcc.1999.1006. [PubMed: 10471354]

34. Gown A, Willingham M. Improved detection of apoptotic cells in archival paraffin sections: immunohistochemistry using antibodies to cleaved caspase 3. J Histochem Cytochem. 2002; 50:449. doi:10.1177/002215540205000401. [PubMed: 11897797]

35. Saeed M, van Dijke CF, Mann JS, et al. Histologic confirmation of microvascular hyperpermeability to macromolecular MR contrast medium in reperfused myocardial infarction. J Magn Reson Imaging. 1998; 8:561–7. doi:10.1002/jmri.1880080308. [PubMed: 9626869]

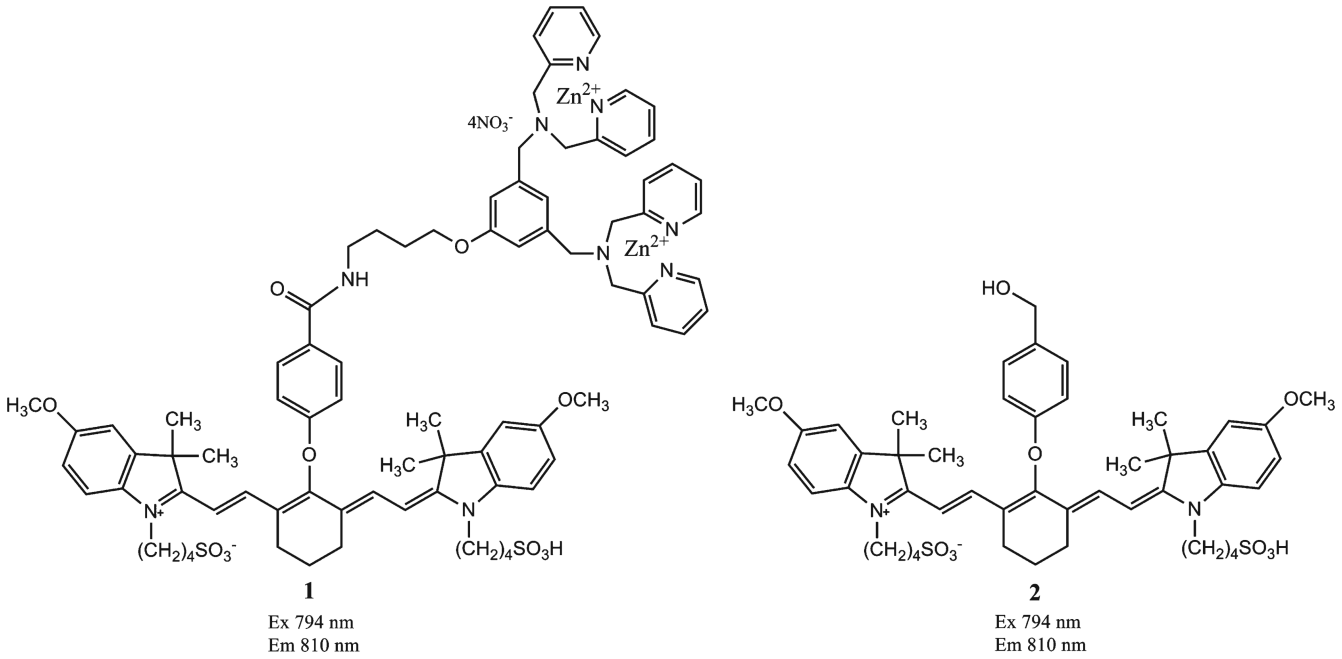

Figure 1.
Chemical structures of PSVue®794 (1) and control dye (2). The compounds exhibit absorbance and fluorescence excitation maximum at 794 nm and emission maximum at 810 nm.

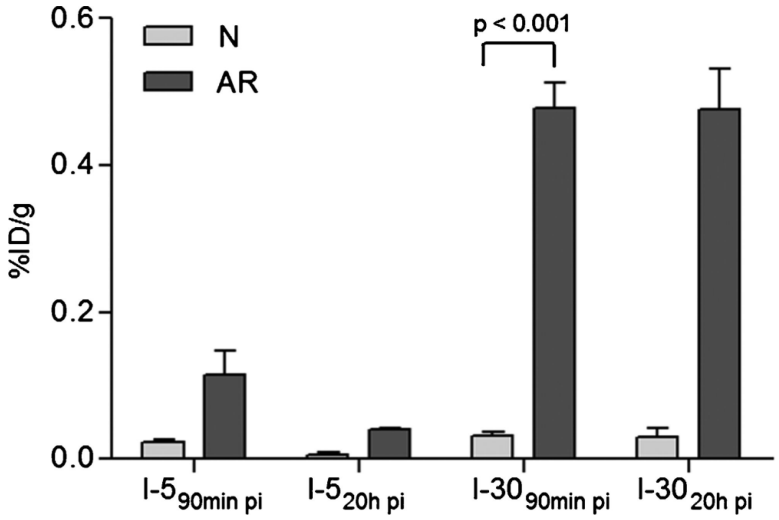

Figure 2.

Uptake of radioactivity (%ID/g) in normal myocardium (N) and area at risk (AR) at 90 minutes (90min pi) or 20 hours (20h pi) postinjection of ^{99m}Tc glucarate in rats subjected to 5 minutes (I-5) or 30 minutes (I-30) ligation of the left coronary artery. Values are presented as mean ± SD, $n = 3$ for I-$5_{90\text{min pi}}$ andr I-$30_{90\text{min pi}}$ and $n = 2$ for I-$5_{20\text{h pi}}$ and I-$30_{20\text{h pi}}$.

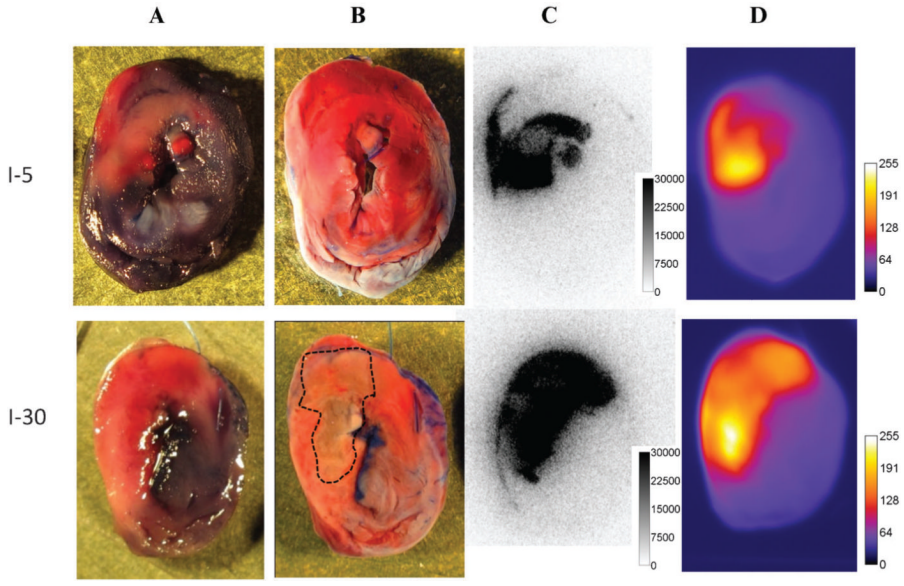

Figure 3.

A, Digital photographs of 2 mm slices of rat hearts subjected to 5 minutes ligation of the left coronary artery (LCA) (I-5) or 30 minutes ligation of the LCA (I-30) and sacrificed 90 minutes following ^{99m}Tc glucarate injection. The area at risk is unstained by Evans blue (*pink areas* in A). *B*, Infarcted areas are visible as TTC-negative (*pale yellow-white*) in I-30 and are marked by a *dashed line*. *C*, Corresponding autoradiograms with regions of high ^{99m}Tc glucarate uptake matching the area at risk and no uptake in normal myocardium. *D*, Fluorescence images of the same myocardial slices showing uptake of compound 1 in the area at risk with topography similar to that of ^{99m}Tc glucarate.

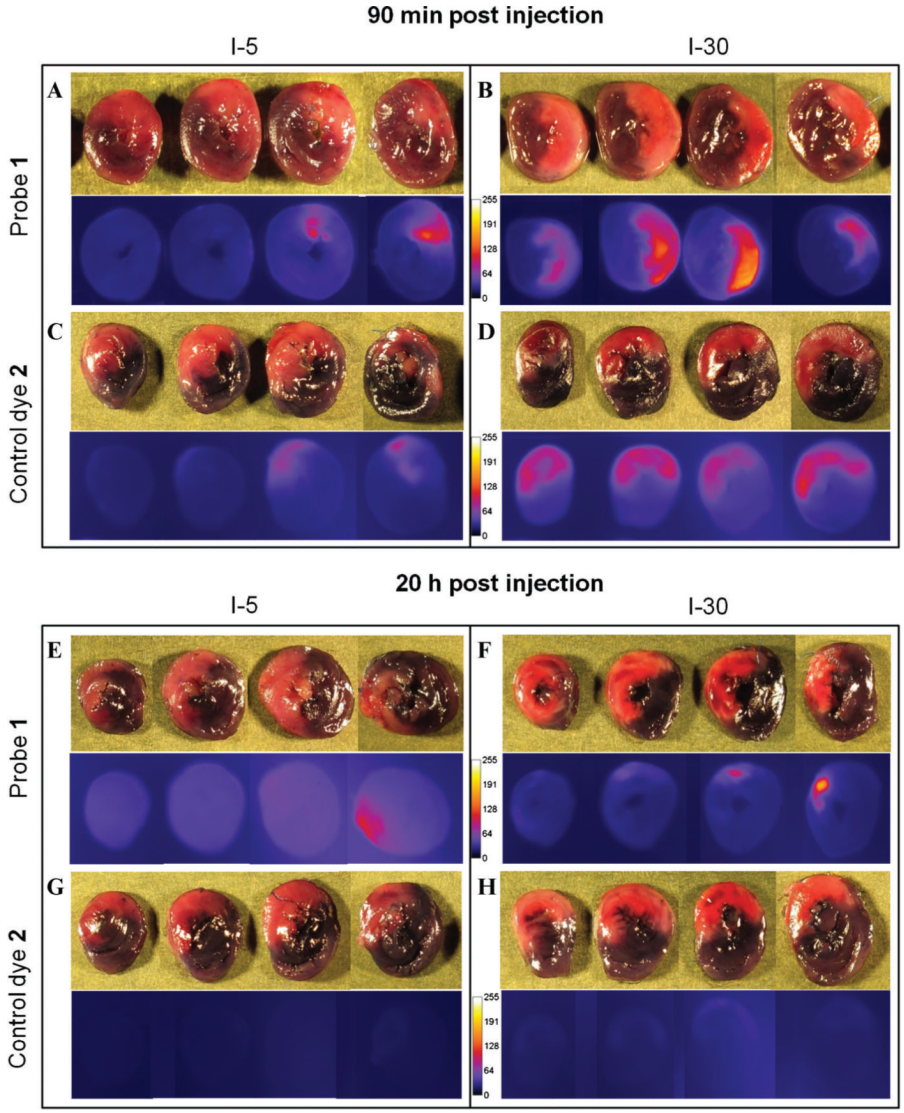

Figure 4.

Fluorescence images of targeting of ischemia-reperfusion injury by compound 1 (A, B, E, and F) or control dye 2 (C, D, G, and H) in hearts subjected to 5 minutes (*left panels*) or 30 minutes (*right panels*) ligation of the left coronary artery. Images were collected at 90 minutes (*upper panels*) or at 20 hours (*lower panels*) postinjection. The area at risk is devoid of Evans blue staining (*pink areas in top rows*). Fluorescence images were thresholded to the same absolute value.

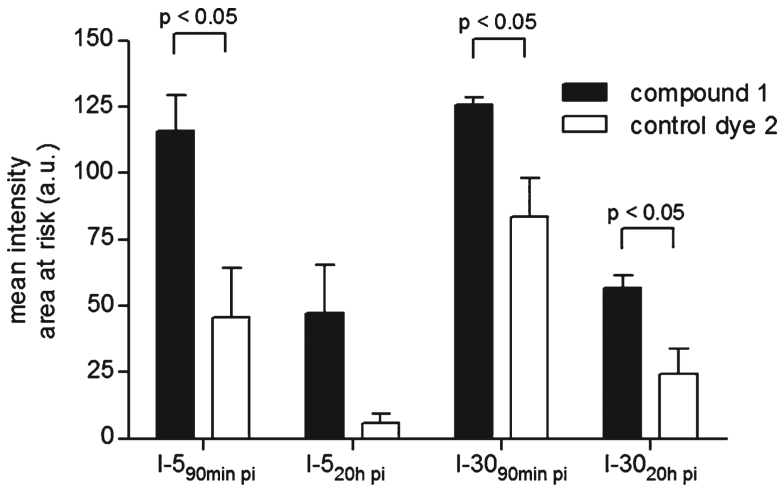

Figure 5.

Ex vivo mean fluorescence intensities in the area at risk of hearts subjected to 30 minutes (I-30) or 5 minutes (I-5) ligation of the left coronary artery at 90 minutes or 20 hours following intravenous injection of compound 1 or control dye 2. Values are presented as mean ± SD. Three rat hearts were used to calculate the mean intensity at each time point.

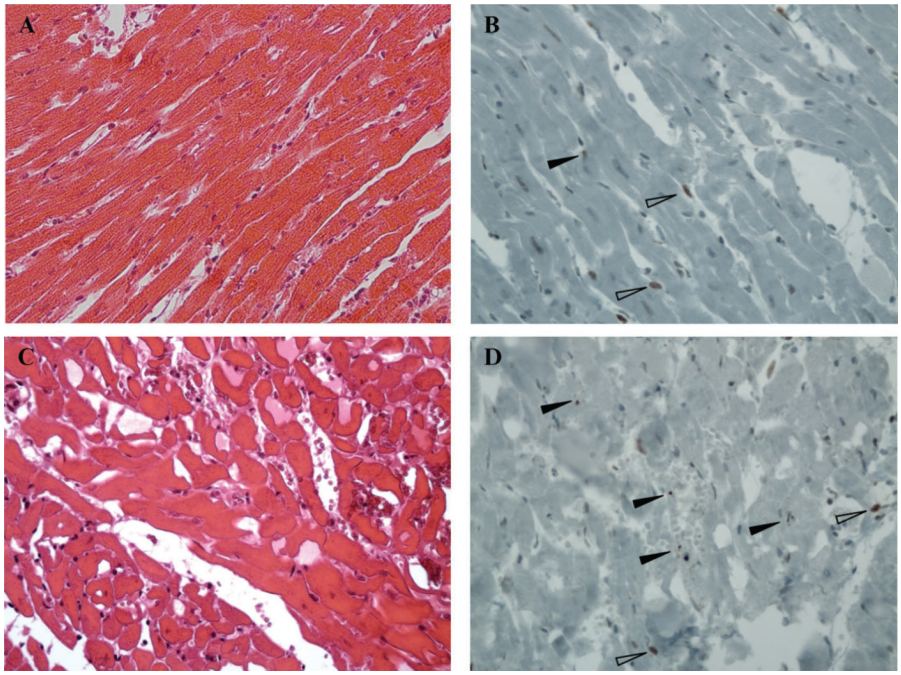

Figure 6.
Representative hematoxylin-eosin staining (A and C) and cleaved caspase-3 immunostaining (B and D) of 3 μm myocardial sections of rats subjected to 5 minutes (A and B) or 30 minutes (C and D) ligation of the left coronary artery (Magnification × 20). *Filled arrows* indicate apoptotic cells. Open arrows indicate positively stained cells with normal nuclear morphology.